

## Structure and magnetic ordering in $\text{CeNi}_x\text{Sn}_2$ compounds

P. Schobinger-Papamantellos<sup>a,\*</sup>, J. Rodríguez-Carvajal<sup>b</sup>, G.H. Nieuwenhuys<sup>c</sup>, L.W.F. Lemmens<sup>c</sup>, K.H.J. Buschow<sup>d</sup>

<sup>a</sup>Laboratorium für Kristallographie, ETHZ, CH-8092 Zürich, Switzerland

<sup>b</sup>Laboratoire Léon Brillouin (CEA-CNRS), Centre d'Etudes de Saclay F91191, Gif-sur-Yvette, France

<sup>c</sup>Kamerlingh Onnes Laboratory, University of Leiden, P.O. Box 9506, NL-2300 RA Leiden, The Netherlands

<sup>d</sup>Van der Waals–Zeeman Institute, University of Amsterdam, Valckeniersstr. 65, NL-1018 XE Amsterdam, The Netherlands

### Abstract

Three  $\text{CeNi}_x\text{Sn}_2$  compounds of different nominal Ni concentrations ( $x = 0.65, 0.75, 0.85$ ) were studied by high resolution neutron diffraction. The refinement of the nuclear structure shows that these compounds are single phase and that the actual compositions are close to the nominal ones. Low temperature neutron data of the  $\text{CeNi}_{0.85}\text{Sn}_2$  compound [refined to  $x = 0.864(2)$ ] confirm the micromagnetic behaviour already observed in a previous sample ( $I$ ) refined to  $x = 0.840(4)$ : coexistence of domains of two distinct magnetic phases in equal amounts. The relative amount of the two domains depends on  $x$ . One of these phases is ferromagnetic,  $\mathbf{q}_1 = 0$  with  $T_C = 3$  K. The other phase is a modulated antiferromagnet (antiphase domain type with two amplitudes) with  $T_N = 4.0$  K. Its magnetic ordering can be described by two propagation vectors  $\mathbf{q}_2 = (010)$  ( $C_p$  magnetic lattice) and  $\mathbf{q}_3 = 1/3\mathbf{b}^*$ . The ordered magnetic moment value at 1.5 K in both phases is  $2.0 \mu_B/\text{Ce}$  atom and the moments point into the same direction, along  $c$ . In sample ( $I$ ) the two phases were present in equal amounts while in the present sample the amount of the ferromagnetic phase is strongly reduced to approximately 16%. The magnetic properties of these compounds and of compounds with higher and lower nominal Ni concentrations have been studied by us in more detail by means of measurements of specific heat, the magnetisation, the AC and DC susceptibility. In several cases two magnetic phase transitions were observed. The nature of these transitions is discussed in the light of the low-temperature neutron diffraction results obtained for the more Ni-rich samples. © 1997 Elsevier Science S.A.

**Keywords:** Rare-earth; Magnetic structure; Neutron diffraction

### 1. Introduction

$\text{CeNiSn}_2$  crystallizes with the  $\text{CeNiSi}_2$  type of structure [1–3] (Cmcm space group  $a = 0.4485$  nm,  $b = 1.774$  nm,  $c = 0.4513$  nm,  $Z = 4$ ). According to Skolozdra et al. [2,3],  $\text{CeNiSn}_2$  forms a range of solid solutions characterized by a different degree of Ni deficiency. It is still an open question whether a

compound having the stoichiometric composition really exists. Francois et al. [4] report the upper limit of  $x$  in  $\text{CeNi}_x\text{Sn}_2$  as 0.74.

Magnetic properties have been reported for apparently stoichiometric  $\text{CeNiSn}_2$  which orders antiferromagnetically below  $T_N^1 = 3.9$  K and which is further characterised by the quantities  $\theta_p = 5$  K and  $\mu_{\text{eff}} = 2.43 \mu_B$  [5]. On the basis of specific heat and magnetic susceptibility measurements [5]  $\text{CeNiSn}_2$  undergoes at 2.6 K a second magnetic phase transition but its Néel temperature is supposed to lie at slightly higher tem-

\* Corresponding author.

peratures ( $T_N^H = 3.2$  K) similarly to the iso-morphic CeNiGe<sub>2</sub> compound. From plots of unit cell volumes vs. atomic number of the lanthanides for the RNiGe<sub>2</sub> and RNiSn<sub>2</sub> series both Ce compounds show no anomaly indicating a valence fluctuation.

In a recent study the magnetic properties of a sample of nominal composition CeNiSn<sub>2.1</sub> (referred to as sample 1 in the following) were studied by magnetisation measurements and neutron diffraction [6,7]. The refinement of 293 K high resolution neutron data shows that this compound is single phase and Ni deficient and contains a small amount of Ni<sub>3</sub>Sn<sub>2</sub>. The corresponding formula is CeNi<sub>0.840(4)</sub>Sn<sub>2</sub>. Surprisingly at 1.5 K two coexisting magnetic phases were observed in equal amounts. One of these is ferromagnetic  $q_1 = 0$  with  $T_C = 3$  K. The other phase is an antiferromagnetic modulated phase (antiphase domain type with two amplitudes) with  $T_N = 4.0$  K. Its magnetic ordering can be described by two propagation vectors  $q_2 = (010)$  ( $C_P$  magnetic lattice) and  $q_3 = 1/3b^*$ . The ordered magnetic moments are equal to 2.0  $\mu_B$ /Ce atom at 1.5 K in both phases and point into the same direction, along  $c$ . Above 2 K the wave vector  $q_3$  becomes incommensurate with the crystal lattice. The observation of two magnetic phases is attributed to the occurrence of concentration fluctuations associated with the Ni deficiency.

In the present investigation we have addressed the effect of the Ni deficiency on the magnetic properties of CeNi<sub>*x*</sub>Sn<sub>2</sub> compounds in more detail by means of magnetic and specific heat measurements. We will show that the magnetic properties are fairly complex for the Ni rich compounds in particular and involve generally more than one magnetic phase transition. In order to exclude the possibility that the effects observed find their origin in the presence of more

than one crystallographic phase, we present also results of high-resolution neutron diffraction performed on several of these compounds.

## 2. Experimental procedures

The powder samples used in this investigation were prepared by arc-melting followed by vacuum annealing at 800°C. In order to suppress Ni–Sn impurity phases as far as possible the samples studied in the present investigation were of the nominal composition CeNi<sub>*x*</sub>Sn<sub>1.9</sub> ( $x = 0.65, 0.75, 0.85$ ). The CeNi<sub>*x*</sub>Sn<sub>2</sub> samples used for the neutron diffraction had the nominal composition  $x = 0.65, 0.75$  and 0.85. Magnetic measurements and specific heat measurements were made also on compounds with Ni concentrations corresponding to  $x = 1.0, 0.50$  and  $x = 0.40$ . The actual composition of the main phase of the samples derived from EPMA analyses has been listed in Table 1.

The neutron data were collected at the facilities of the Orphée reactor (LLB-Saclay). The 293 K data were collected with the two-axes high resolution instrument 3T2 (20 detectors,  $\lambda = 1.227$  Å in the  $2\theta$  range 0–125.45°). The step increment in  $2\theta$  was 0.05°. Low temperature (1.5 K and 10 K) data were collected for the compound CeNi<sub>0.85</sub>Sn<sub>2</sub> with the G42 spectrometer ( $\lambda = 2.34186$  Å in the  $2\theta$  range 0–170° with the step increment in  $2\theta$  0.1°). The data were evaluated by the program Fullprof [8].

## 3. Results and discussion

### 3.1. Crystal structure of CeNi<sub>*x*</sub>Sn<sub>2</sub> ( $x = 0.85, 0.75, 0.65$ ) from 293 K neutron data

Results of the high resolution neutron data ob-

Table 1  
Crystallographic and magnetic characteristics of several CeNi<sub>*x*</sub>Sn<sub>2</sub> compounds

<i>x</i>	<i>x</i> EPMA	<i>x</i> neutron	<i>a</i> (nm)	<i>b</i> (nm)	<i>c</i> (nm)	<i>T</i> <sub>1</sub> (K)	<i>T</i> <sub>2</sub> (K)
1	0.91		0.4483	1.7934	0.4493	2.2	3.8
0.85	0.89	0.840(4)	0.44835(2)	1.79149(6)	0.45039(2)	3.0	4.0
			0.4503	1.7970	0.4475		(4.6)
0.75	0.77	0.864(4)	0.44795(2)	1.79262(8)	0.45017(2)		
			0.4495	1.7705	0.4492	2.3	[4.0]
0.65	0.69	0.780(4)	0.44942(2)	1.77799(5)	0.44968(2)		
			0.4514	1.7549	0.4489	1.4	
0.50	0.54	0.668(4)	0.45148(1)	1.75791(6)	0.44832(1)		
0.40	0.45		0.4524	1.7320	0.4480	1.6	
			0.4529	1.7204	0.4468	1.9	

Notes: The magnetic transition temperatures of the compounds for which the composition  $x$  is specified by EPMA analysis were determined from AC susceptibility measurements.

Transition temperatures given between parentheses or square brackets refer to DC susceptibility measurements or specific heat measurements, respectively.

The lattice parameters were derived from X-ray diffraction.

Refined composition values  $x$  and lattice parameters are listed for the compounds investigated by high resolution neutron diffraction.

The transition temperatures of the compound with the refined composition  $x = 0.84$  were derived from neutron data made at various temperatures [7].

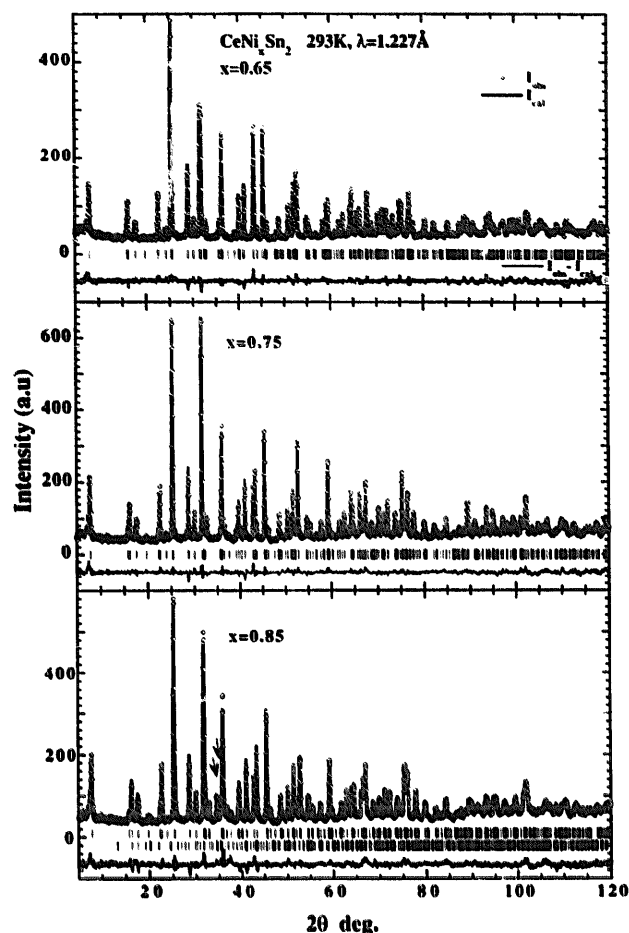


Fig. 1. Observed and calculated neutron intensities of three samples of nominal composition  $\text{CeNi}_x\text{Sn}_2$  ( $x = 0.65, 0.75, 0.85$ ) in the paramagnetic state at 293 K. The arrows indicate the strongest nuclear reflections of coexisting  $\text{Ni}_3\text{Sn}_2$  (1.3% weight) present in the sample  $x = 0.85$ .

tained at 293 K are shown in Fig. 1. The refinement results led, within the  $3\sigma$  limit, to the same Ni concentrations as obtained by the metallurgical analysis and has also been included in Table 1. A small

Table 2  
Refined parameters from 293 K neutron data of  $\text{CeNi}_x\text{Sn}_2$  samples of nominal composition  $x = 0.85, 0.75, 0.65$

Parameter	$x = 0.65$	$x = 0.75$	$x = 0.85$	$x = 1$
$y_{\text{Ce}}$	0.1063(1)	0.10678(1)	0.10778(2)	0.1069(2)
$B_{\text{Ce}} \text{ (nm)}^2$	0.0086(4)	0.0090(4)	0.0127(5)	0.0148(6)
$y_{\text{Ni}}$	0.3154(1)	0.31680(8)	0.31756(1)	0.3172(1)
$B_{\text{Ni}} \text{ (nm)}^2$	0.0143(5)	0.0121(4)	0.0136(4)	0.0133(5)
$oc_{\text{Ni}}$	0.668(4)	0.780(4)	0.864(4)	0.840(4)
$y_{\text{Sn1}}$	0.4502(1)	0.4519(1)	0.4526(1)	0.4517(1)
$B_{\text{Sn1}} \text{ (nm)}^2$	0.0234(5)	0.0204(4)	0.0186(6)	0.0195(6)
$y_{\text{Sn2}}$	0.74998(1)	0.74939(2)	0.7491(2)	0.7494(1)
$B_{\text{Sn2}} \text{ (nm)}^2$	0.0100(4)	0.0084(3)	0.0062(4)	0.0035(6)
$R_p\%, R_w\%$	8.27, 13.9	7.57, 12.6	8.5, 14.4	4.1, 13.0
$R_{\text{exp}}\%, \chi^2$	9.67, 2.02	8.26, 2.52	8.26, 3.04	9.18, 2.02

Note: The last column refers to a compound with the nominal composition  $\text{CeNiSn}_2$  [7].

correction for preferential orientation of the powder particles was included in the refinement. The latter was found to be associated with the plate-like shape of the powder particles perpendicular to the  $b$ -axis. The refined structural parameters are summarized in Table 2.

The high-resolution neutron results confirm the  $\text{CeNiSi}_2$  type of structure reported already by various authors [1–4] and clearly show the existence of an homogeneity range of  $\text{CeNi}_x\text{Sn}_2$  with respect to the Ni content. In fact, Skolozdra and Komarovskaya [3] and also Francois et al. [4] had advocated before that the occurrence of  $3d$  atom deficiencies is quite common in ternary rare earth silicides, germanides and stannides of the  $\text{CeNiSi}_2$  type of structure.

From the high resolution neutron diffraction patterns obtained at 293 K shown in Fig. 1 can be seen that up to high diffraction angles, no line splitting or any unusual line broadening occurs that would have been indicative of phase separation.

Within the limits of the instrumental resolution, this neutron diffraction study provides a quantitative characterization of the samples which is in satisfactory agreement with the results of the metallographic analyses. Most importantly, it proves the existence of only a single Ni deficient of  $\text{CeNi}_x\text{Si}_2$ -type phase in these samples. The  $x = 0.85$  sample with refined composition  $\text{CeNi}_{0.864(4)}\text{Sn}_2$  contains 1.3% (weight) of the non-magnetic impurity phase  $\text{Ni}_3\text{Sn}_2$ .

### 3.2. Magnetic structure of $\text{CeNi}_{0.864(2)}\text{Sn}_2$ at 1.5 K

The 1.5 K temperature neutron data (Fig. 2) of the compound with refined composition  $\text{CeNi}_{0.864(2)}\text{Sn}_2$  comprise only a few weak resolved magnetic reflections in the low  $2\theta$  range similarly to the previously studied sample of refined composition  $\text{CeNi}_{0.840(4)}\text{Sn}_2$  (I). These reflections are better visible in the difference diagram (1.5–10 K). For brevity, we refer for an extensive description of the experimental facts of sample I to our earlier report [7]. As already given in Sec. 1 the data analysis of the magnetically ordered state (see Fig. 2) consists of three sets of reflections comprising ferromagnetic ( $q_1 = 0$ ) and antiferromagnetic [ $q_2 = (010)$ ,  $q_3 = 1/3b^*$ ] reflections. The refinement of the 1.5 K magnetic intensities confirmed the coexistence of domains having the same type of ferromagnetic and antiferromagnetic structures as in the sample with  $x = 0.840(4)$ . Results are given in Table 3. The refined ferromagnetic  $\mu_z = 0.8(1)$  moment component is reduced by almost a factor of two compared to the sample with  $x = 0.84$ . This means that the amount of the ferromagnetic phase is reduced in favour of the antiphase domain antiferromagnetic phase. A rough estimate of the relative amounts of the two magnetic phases can be achieved

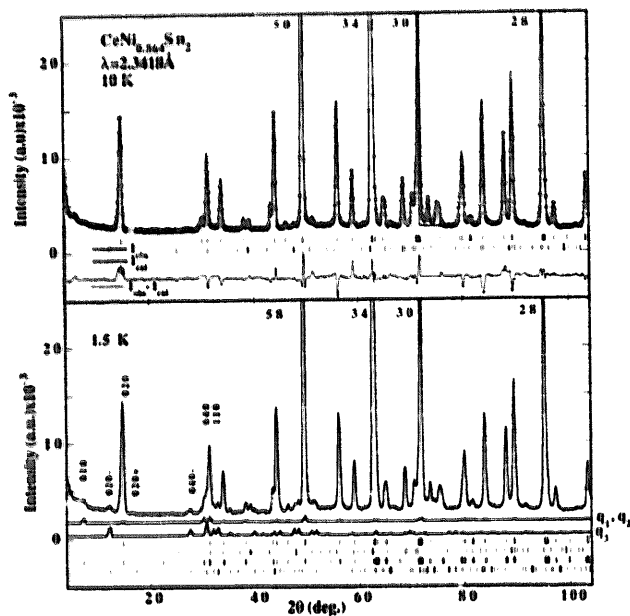


Fig. 2. A part of the observed and calculated neutron intensities of  $\text{CeNi}_{(1-x)\text{Sn}_x}\text{Sn}_2$ : (a) in the paramagnetic state at 10 K (top part); (b) in the magnetically ordered state at 1.5 K. The calculated ferromagnetic and the antiferromagnetic profile intensities pertaining to the wave vectors ( $q_1 = 0$ ,  $q_2 = 010$ ,  $q_3 = 1/3b^*$ ) are drawn separately below the  $I_{\text{obs}}$  pattern (bottom part).

by assuming that Ce has the same moment value 2.0  $\mu_B$  as in sample 1. Then the volume of the present ferromagnetic phase would correspond to  $(0.8/2.0)^2 = 16\%$  and that of the antiferromagnetic phase 84%.

### 3.3. Specific heat and magnetic measurements

Results of the specific heat measurements are displayed in Fig. 3. Well defined peaks, indicative of magnetic phase transitions in the temperature range considered, are observed only in the compounds with Ni concentrations corresponding to the EPMA values  $x = 0.91, 0.77$  and  $0.54$ . In the compound with  $x = 0.69$  there is only a small hump and in the compound with  $x = 0.77$  there is a pronounced shoulder on the high-temperature side of the main peak. All these thermal events have been marked by arrows in Fig. 3.

Additional information as to the occurrence of magnetic phase transitions was obtained from measurements of the temperature dependence of the AC and DC susceptibility. The results of the former measurements in particular were most revealing because here the phase transitions showed up as sharp peaks, such as shown for the compound with  $x = 0.77$  in Fig. 4. The peak temperature, 2.3 K, has been listed in Table 1, together with those found from AC susceptibility measurements on the other compounds investigated. Two temperatures have been listed when two peaks were observed, as in the case of the compound with  $x = 0.91$ . We have also listed in this table any

Table 3

Refined structural parameters of the  $\text{CeNi}_{0.85}\text{Sn}_2$  compound in the paramagnetic state at 10 K and in the magnetically ordered state at 1.5 K

Parameter	Temperature	
	10 K	1.5 K
$y_{\text{Ce}}$	0.1065(3)	0.1065(3)
$y_{\text{Ni}}$	0.3168(1)	0.3168(1)
$oc_{\text{Ni}}$	0.864(4)	0.864(4)
$y_{\text{Sn1}}$	0.4513(2)	0.4513(2)
$y_{\text{Sn2}}$	0.7481(2)	0.7481(2)
$\mu_2 [\mu_B]$ (set I)	—	0.8(1)
$\mu_{12} [\mu_B]$ (set II)	—	0.22(3)
$\mu_{13} [\mu_B]$ (set III)	—	2.09(8)
$a$ (nm)	0.44641(1)	0.44639(2)
$b$ (nm)	1.78923(7)	1.78911(8)
$c$ (nm)	0.44883(2)	0.44880(2)
$B_{\text{of}}$ (nm) <sup>2</sup>	0.014(5)	0.014(5)
$R_p\%$ , $R_{m1}\%$ , $R_{m2}\%$	3.96, —, —	5.02, 12.7, 25
$R_{\text{wp}}\%$ , $R_{\text{exp}}\%$ , $\chi^2$	12.4, 3.1, 15	12.5, 3.24, 15

Notes:  $\mu_2$  is the ferromagnetic moment value ( $q_1 = 0$ ).

$\mu_{12} = \mu_{1/2}$  is the antiferromagnetic moment value [ $q_2 = (010)$ ].

$\mu_{13}$  is the Fourier component giving rise to the transversal amplitude modulated structure along  $c$  ( $q_3 = 1/3b^*$ ).

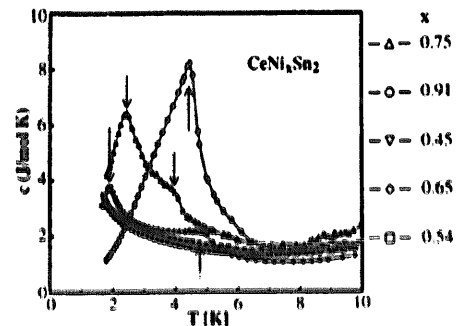


Fig. 3. Temperature dependence of the specific heat  $C_p$  of various  $\text{CeNi}_x\text{Sn}_2$  compounds. The arrows mark possible magnetic phase transitions.

additional information on magnetic transition temperatures not observed by ac susceptibility measurements but showing up as thermal events in the specific heat data or in the DC susceptibility.

More information on the nature of the phase transitions was obtained from the DC susceptibility data. The results shown for the compound with  $x = 0.77$  in Fig. 5 clearly identify the peak shown in Fig. 4 as belonging to the onset of antiferromagnetic ordering.

However, the DC susceptibility peak has the tendency to disappear when the measuring fields become too large. Most likely this behaviour originates from the fact that this single phase sample, due to concentration fluctuations, gives rise to two magnetic phases. In analogy with neutron diffraction results obtained by us [6,7] for the more Ni rich compounds, such as sample 1 with  $x = 0.840$  and the present sample with

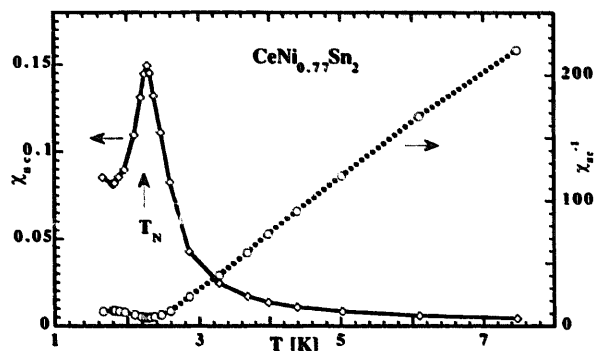


Fig. 4. Temperature dependence of the AC susceptibility of the compound with  $x = 0.77$ .

$x = 0.864$ , one may assume that one of these phases is characterised by long range antiferromagnetic ordering. The second magnetic phase may be a cluster glass showing no long-range magnetic order below the Néel temperature of the first magnetic phase but does give rise to long-range ferromagnetic order at temperatures much lower than  $T_N$ . Indications for the onset of short range magnetic ordering of the second phase may be obtained from the results of the specific heat measurements shown in Fig. 3 where one notices a pronounced shoulder at approx. 4 K on the high-temperature side of the peak. Indications that the second magnetic phase shows a tendency to become ferromagnetically ordered at much lower temperatures can be obtained from the shape of the field dependence of the magnetisation measured at various temperatures and shown in Fig. 6. The hysteresis loop measured at the lowest temperature considered is seen in Fig. 7 to display remanence and hysteresis. Presumably the magnetic phase with long-range ferromagnetic ordering contributes little to the magnetisation and is the constricted-loop behaviour representative of a ferromagnet in which reversed magnetic domains can be nucleated very easily. Here one has to bear in mind that the ferromagnetic phase and the antiferromagnetic phase form a coherent crystallographic lattice and that the interface between these

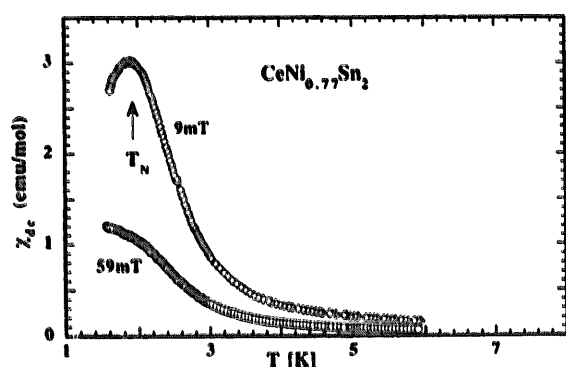


Fig. 5. Temperature dependence of the DC susceptibility of the compound with  $x = 0.77$ , measured in fields of 9 mT and 59 mT.

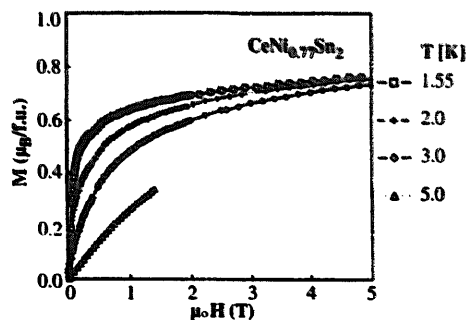


Fig. 6. Field dependence of the magnetisation of the compound with  $x = 0.77$ , measured at various temperatures.

two phases forms an almost ideal location for the nucleation of Bloch walls.

A verification of the interpretation of the magnetic and specific heat measurements has to come from further neutron diffraction studies which we plan to perform in the low-temperature range in the near future. Because it is difficult to interpret the magnetic data in a quantitative way, we hope to obtain information from further neutron diffraction studies as to how the relative amounts of the phase with long-range antiferromagnetic order and the ferromagnetic phase vary with Ni concentration. This would eventually allow us to reach a conclusion as to which of these two magnetic phases is the more Ni deficient one. It appears that the micromagnetic behaviour is common to this family of compounds due to fluctuations of the Ni concentration. The results obtained concerning the domain distribution in the two samples with refined compositions  $x = 0.840(4)$  and  $x = 0.864(2)$  indicate that an increase of the Ni content by an amount as small as 2.5% strongly increases the relative amount of the antiferromagnetic phase. One may wonder whether the same magnetic phases will persist at lower  $x$  values and whether changes in  $x$  will affect the domain distribution in the same way as for the Ni rich phases.

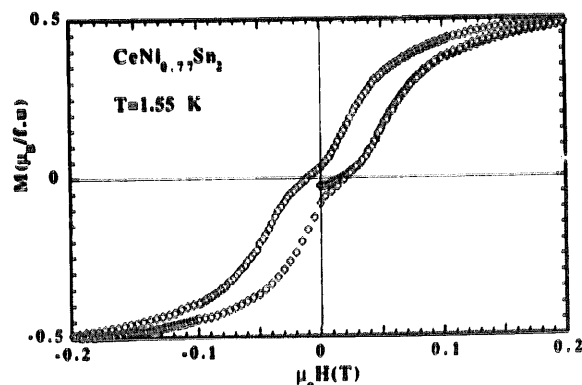


Fig. 7. Hysteresis loop of the compound with  $x = 0.77$  measured at 1.55 K.

**References**

- [1] O.P. Bodak, E.I. Gladyshevskii, *Sov. Phys. Crystallogr.* 14 (1970) 859.
- [2] R.V. Skolezdra, L. Komarovskaya, *Izv. Akad. Nauk SSSR Met.* 2 (1988) 214.
- [3] R.V. Skolezdra, L. Komarovskaya, *Russ. Metall. Met.* 2 (1988) 207.
- [4] M. Francois, G. Venturini, B. Malaman, B. Roques, *J. Less Common Met.* 160 (1990) 197.
- [5] V.K. Pecharsky, K.A. Gscheidner, Jr, L.L. Miller, *Phys. Rev. B* 43 (1991) 10906.
- [6] P. Schobinger-Papamantellos, J. Rodríguez-Carvajal, K.H.J. Buschow, *J. Alloys Comp.* 240 (1996) 85–87.
- [7] P. Schobinger-Papamantellos, J. Rodríguez-Carvajal, K. Prokes, K.H.J. Buschow, *J. Cond. Mat.* 8 (1996) 8635.
- [8] J. Rodríguez-Carvajal, *Physica B* 192 (1993) 55.